Urania
Jurnal Ilmiah Daur Bahan Bakar Nuklir

Beranda jurnal: https://ejournal.brin.go.id/urania/

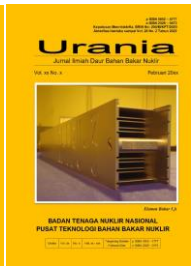


# ANALYSIS OF DENSITY, PHASE, AND MICROSTRUCTURE IN U–Mo ALLOYS

**Saga Octadamailah[1], Ganisa Kurniati Suryaman[1], Supardjo[1], Deni Mustika[1], Juan Carlos Sihotang[1], Yusuf Gigih Wicaksono[1], Slamet Pribadi[2], Boybul[1], Anissa Isnaini[1], Ratih Langenati[1], Dede Sutarya[1]**

[1]Research Center for Nuclear Materials and Radioactive Waste Technology – BRIN
KST B.J. Habibie, Building 720, Serpong, Tangerang Selatan, Banten, Indonesia 15314
[2]Directorate of Nuclear Facilty Management – BRIN
KST B.J. Habibie, Building 30, Serpong, Tangerang Selatan, Banten, Indonesia 15314
Email: saga.octadamailah@brin.go.id

(Submitted: 04–12–2024, Revised: 23–01–2025, Accepted: 03–02–2025)

**ABSTRACT**

**ANALYSIS OF DENSITY, PHASE, AND MICROSTRUCTURE IN U–Mo ALLOYS.** The performance of research reactors heavily depends on the intensity of the neutron flux produced, which is a key factor in reactor efficiency and effectiveness. To enhance the performance of research reactors, high-density fuel is required to increase neutron flux in the reactor core, enabling optimal irradiation processes. One of the most promising fuel candidates is uranium-molybdenum (U-Mo) alloy. This study aims to investigate the properties of U-Mo alloys through a series of characterizations, including density measurements, phase analysis using X-ray Diffraction (XRD), and microstructural observations using a Scanning Electron Microscope (SEM). The density measurements revealed values close to theoretical calculations, with densities of 17.423 g/cm³ for U-7Mo, 17.292 g/cm³ for U-8Mo, and 17.229 g/cm³ for U-9Mo. XRD analysis identified the presence of the γ-U phase with a body-centered cubic (bcc) crystal structure, characterized by diffraction peaks at 2θ angles of 37°, 53°, 66°, and 78°. SEM observations showed a pattern of bright and dark areas, which were further analyzed using Energy Dispersive Spectroscopy (EDS). EDS analysis indicated that the bright areas had a higher concentration of Mo and a lower oxide content compared to the dark areas. These findings suggest that the addition of Mo not only improves the structural homogeneity but also enhances the oxidation resistance of U-Mo alloys.

**Keywords**: U-Mo, neutron flux, phase, research reactor, microstructure.

## INTRODUCTION

Research reactors are facilities widely used in various fields of research, ranging from nuclear physics to irradiation testing for nuclear materials and new fuels [1]. Additionally, research reactors are used for radioisotope production, both for medical and industrial applications [2]. The performance of a research reactor is highly influenced by the intensity of the neutron flux it generates. To achieve a high neutron flux, an increase in the density of fuel containing fissile material, such as Uranium-235, is typically required. Pure uranium, with density of 19 g/cm³, is theoretically an attractive option due to its high atomic density, which allows for an increased number of uranium atoms within a given volume, potentially enhancing neutron production. However, the use of pure uranium as nuclear reactor fuel presents several challenges. Uranium is highly reactive with oxygen and is even pyrophoric, easily ignited upon exposure to air, making its handling quite difficult [3]. Moreover, at high temperatures, uranium undergoes swelling, which can lead to dimensional changes in the fuel [4], posing risks to the structural integrity of the fuel and affecting coolant flow rates within the reactor core.

Several types of uranium alloys have been developed to address these shortcomings. One particularly promising alloy is uranium-molybdenum (U-Mo) [5]. Molybdenum (Mo), as an alloying element, possesses excellent thermal and mechanical properties, including high thermal conductivity that aids in heat dissipation from the fuel, high melting point, large elastic modulus, and low thermal expansion [6]. Additionally, the addition of Mo can minimize oxidation [7]. The combination of these superior properties makes U-Mo alloy a potential fuel for next-generation research reactors. Using U-Mo-based alloys, the fuel density can be increased to approximately 8 gU/cm$^3$ [8]. This increase in density extends the fuel's residence time in the reactor core, reducing the frequency of fuel replacement and indirectly improving the reactor's operational economics [9]. High-density fuel also enables higher burnup, ultimately reducing the volume of radioactive waste produced [10].

Based on previous research [11], γ-U phase is the most stable uranium phase under irradiationi. The addition of Mo enhances the stability of the γ-U phase and improves the overall properties of the alloy [11].

The phase diagram of the U-Mo alloy shown in Figure 1 indicates that the addition of Mo up to 40 at.% (approximately 16 wt.%) can expand the stability range of the γ-U phase. The Mo content in U-Mo fuel candidates typically ranges between 6-10 wt.% [13]. However, excessive Mo addition can reduce the density of the U-Mo alloy.

This study aims to examine the relationship between density, phase, and microstructure in U-Mo alloys. By varying the Mo content to 7, 8, and 9 at.%, the research seeks to determine the optimal composition that provides the best physical and mechanical properties, making it suitable for application as nuclear fuel in research reactors. Specifically, this alloy is expected to serve as an alternative fuel for the G.A. Siwabessy Multipurpose Reactor (RSG-GAS) in the future. The characterization in this study will include microstructural analysis, density measurements, and phase identification.

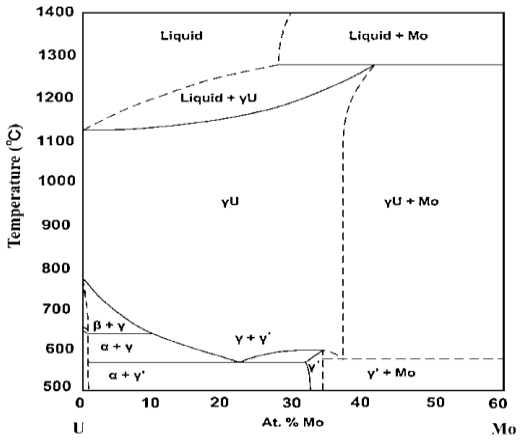


Figure 1. Equilibrium binary phase diagram of U-Mo system [12].

## METHODOLOGY.

The fabrication of U-Mo alloys began with the weighing process. Uranium (U) and molybdenum (Mo) metals were first weighed according to the desired composition ratio. The target mass of the ingot was 20 grams. The detailed mass composition is shown in Table 1.

To remove oxides and impurities from the surface, the U metal underwent pickling using nitric acid ($HNO_3$) and then dried. Afterward, U and Mo metals were placed into an arc melting furnace for the melting process.

 DOI: https://doi.org/10.55981/Urania.2025.10793

The furnace chamber was first filled with an inert gas to prevent oxidation during melting. The electric current was set to 150 A to ensure a sufficiently high temperature for complete melting. This melting process was repeated five times to achieve a homogeneous alloy. After the melting process was completed, the formed U-Mo alloy ingot was slowly cooled and then cut into small specimens. These specimens were subsequently used for various tests to evaluate the material properties of the U-Mo alloy.

The tests conducted included density measurement using an automatic gas pycnometer, phase identification using an X-ray diffractometer (XRD), and microstructure analysis using a scanning electron microscope (SEM).

Table 1. The calculated mass composition data of elements in the fabrication of U-Mo alloys.

| Alloy | Mass (gram) | | |
|---|---|---|---|
| | U | Mo | Total |
| U-7Mo (7 at.% Mo) | 18.60 | 1.40 | 20.00 |
| U-8Mo (8 at.% Mo) | 18.40 | 1.60 | 20.00 |
| U-9Mo (9 at.% Mo) | 18.20 | 1.80 | 20.00 |

## RESULTS AND DISCUSSION

The weighing results of U and Mo metals are listed in Table 2, which shows a difference between the theoretical calculations and the actual weighing results. Although there is a discrepancy, it is relatively small and not significant. Based on the obtained composition, the theoretical density of the metal mixture can be calculated. This theoretical density value is then compared with the density measured using an automatic gas pycnometer. The comparison between the theoretical calculations and the measured density can be seen in Table 3.

The α-U and γ-U phases have different crystal structures, which result in density differences between them. The density of the γ-U phase is lower than that of the α-U phase, with a value of approximately 17.94 g/cm³. In Table 3, the theoretical density calculation is based on the assumption that uranium formed after the melting process is entirely in the γ-U phase. Although there is a difference between the calculated and measured density values, the discrepancy is less than 1%, which is still considered acceptable. This difference is primarily due to the difficulty of obtaining material samples with perfectly accurate weights during the weighing process. The insignificant discrepancy between the theoretical and measured density results suggests that the assumption of uranium being in the γ-U phase after melting is valid. This assumption will be further confirmed through phase identification using XRD to ensure that the uranium in the alloy is indeed in the γ-U phase.

The XRD pattern for U-Mo ingots is shown in Figure 2, where four diffraction peaks are detected at 2θ angles of 37°, 53°, 66°, and 78°. Based on analysis using Highscore software, the identified phase in this alloy is the γ-U phase, which has a body-centered cubic (BCC) crystal structure and belongs to space group number 229. The detected diffraction peaks correspond to crystallographic planes within the BCC structure. The diffraction peak intensities for the (0 0 2), (1 1 2), and (0 2 2) planes are relatively low, whereas only the (0 1 1) plane exhibits a significantly high peak intensity. This was because the samples tested in the XRD instrument were in a solid form. Solid samples tend to have preferred orientations within their crystal structure, which in this case results in a dominant orientation along the (0 1 1) plane. This preferential orientation causes the peak intensity of the (0 1 1) plane to appear more pronounced compared to other planes.

Table 2. Mass composition data of metal elements from weighing in U-Mo alloy fabrication.

| Alloy | U | | Mo | | Ingot |
|---|---|---|---|---|---|
| | mass (gram) | content. (wt.%) | mass (gram) | content (wt.%) | mass (gram) |
| U-7Mo a | 18.5043 | 92.97 | 1.3992 | 7.03 | 19.8867 |
| U-7Mo b | 18.5631 | 93.02 | 1.3921 | 6.98 | 19.9256 |
| U-8Mo a | 18.3098 | 92.00 | 1.5911 | 8.00 | 19.9057 |
| U-8Mo b | 18.3005 | 92.00 | 1.5907 | 8.00 | 19.8551 |
| U-9Mo a | 17.3205 | 90.97 | 1.7196 | 9.03 | 19.0234 |
| U-9Mo b | 18.9795 | 91.01 | 1.8752 | 8.99 | 20.8568 |

Table 3. Calculation and Measurement Results of U-Mo Alloy Density.

| Alloy | Element composition | | Theoretical density ($g/cm^3$) | Measured density ($g/cm^3$) |
|---|---|---|---|---|
| | U | Mo | | |
| U-7Mo | 93% | 7% | 17.3653 | 17.4228 |
| U-8Mo | 92% | 8% | 17.2832 | 17.2917 |
| U-9Mo | 91% | 9% | 17.2011 | 17.2291 |

The U-Mo alloy consists of U and Mo elements. However, in Figure 2, no diffraction peaks other than those belonging to the γ-U phase were observed. This indicates that Mo does not exist as a separate phase but has completely merged with U, forming a homogeneous U-Mo alloy. In other words, Mo is dissolved within the U crystal structure, resulting in only the γ-U phase being detected in the diffraction pattern.

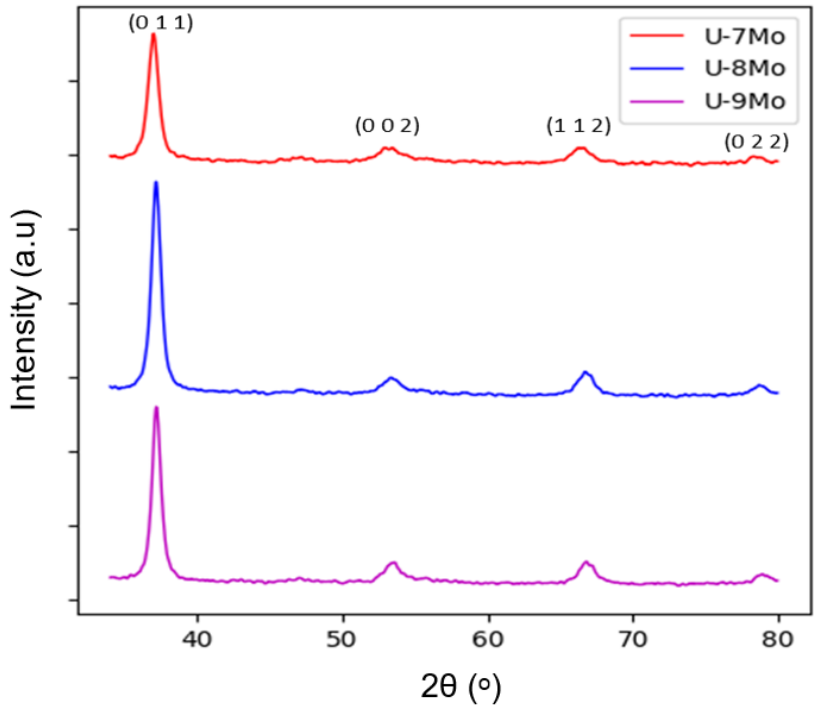


Figure 2. XRD pattern of U-Mo alloy

A more detailed observation of the XRD pattern, as shown in Figure 3, reveals a shift in the 2θ angle to the right as the Mo content in the U-Mo alloy increases. This shift indicates a change in the crystal lattice parameters. According to Bragg's Law ($n\lambda = 2d \sin\theta$) [15], shift to the right suggests that the interplanar spacing, or lattice parameter, has contracted. With a smaller crystal size, more crystallographic planes become detectable, which is marked by an increase in the intensity of the (0 1 1) plane as the Mo content increases. This phenomenon indicates that the addition of Mo not only alters the lattice structure but also facilitates the formation of the γ-U phase. Thus, Mo plays a crucial role in stabilizing the γ-U phase in the U-Mo alloy, enhancing the tendency of the alloy structure to remain in this phase.

The microstructural observations using SEM, as shown in Figure 4, reveal that grain boundaries are not clearly visible, making grain size measurement impossible. However, in general, two distinct color patterns can be observed in the microstructure: bright and dark regions. Elemental composition analysis with energy dispersive spectroscopy (EDS) was performed to identify the elemental distribution within the bright and dark areas, providing a more detailed characterization of the microstructure.

 DOI: https://doi.org/10.55981/Urania.2025.10793

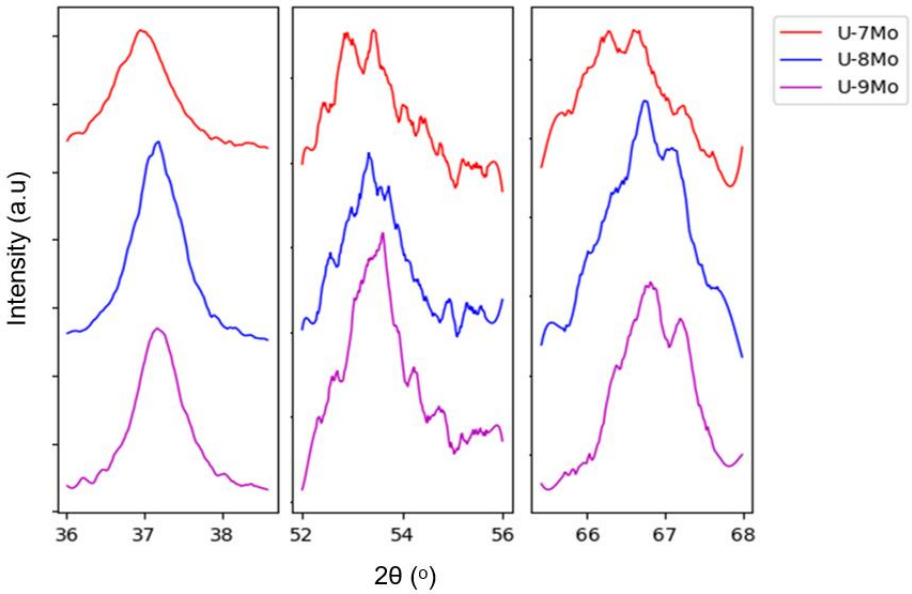


Figure 3. XRD pattern of U-Mo alloy on (0 1 1), (0 0 2), and (1 1 2) plane.

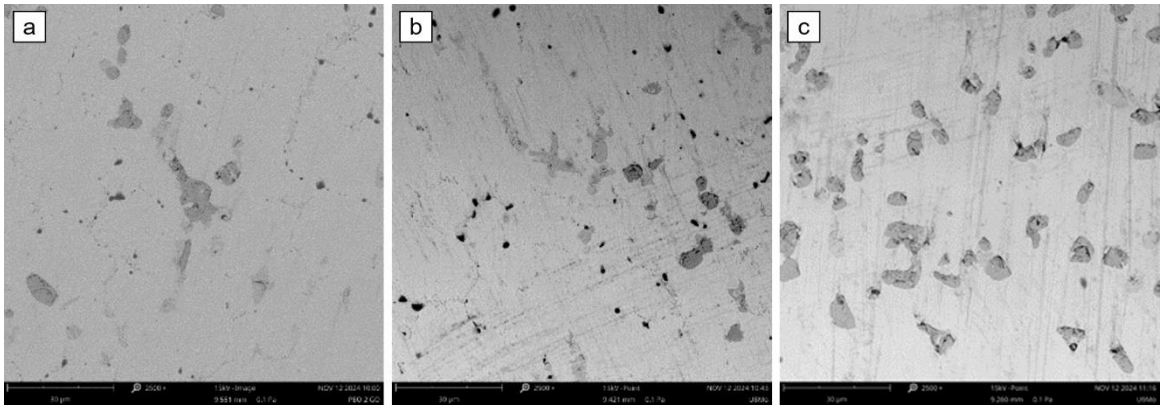


Figure 4. Microstructure observation of U-7Mo (a), U-8Mo (b), and U-9Mo ingot (c) using SEM.

The results of elemental composition measurements using SEM-EDS are shown in Figure 5. The scanning method used was point scanning. The red dots in the upper right images of Figures 5a and 5b indicate the positions where the scans were performed. A significant difference in elemental composition between the bright and dark regions is evident. In the bright regions (Figure 5a), the Mo content is higher compared to the dark regions (Figure 5b). This indicates that the distribution of Mo in the U-Mo alloy is not yet fully uniform, as darker areas still contain lower Mo concentrations. A similar bright-dark pattern has also been observed in the fabrication of monolithic U-Mo fuel [16]. The uneven Mo distribution suggests that the homogenization process was not entirely optimal, highlighting the need for further processing to achieve a more uniform element distribution within the alloy.

SEM-EDS analysis also revealed the presence of oxygen (O). The dark regions exhibited significantly higher oxide content compared to the bright regions. These oxides formed due to the interaction of the sample with the etching solution during the preparation process. In the bright regions, where the Mo content was higher, oxygen was detected in lower amounts. Conversely, in the dark regions, where the Mo content was lower, oxygen was more dominant. This phenomenon suggests that Mo addition not only acts as a stabilizer for the γ-U phase but also reduces oxidation reactivity in the alloy. With higher Mo content, the alloy exhibits a more stable microstructure and is less prone to oxidation.

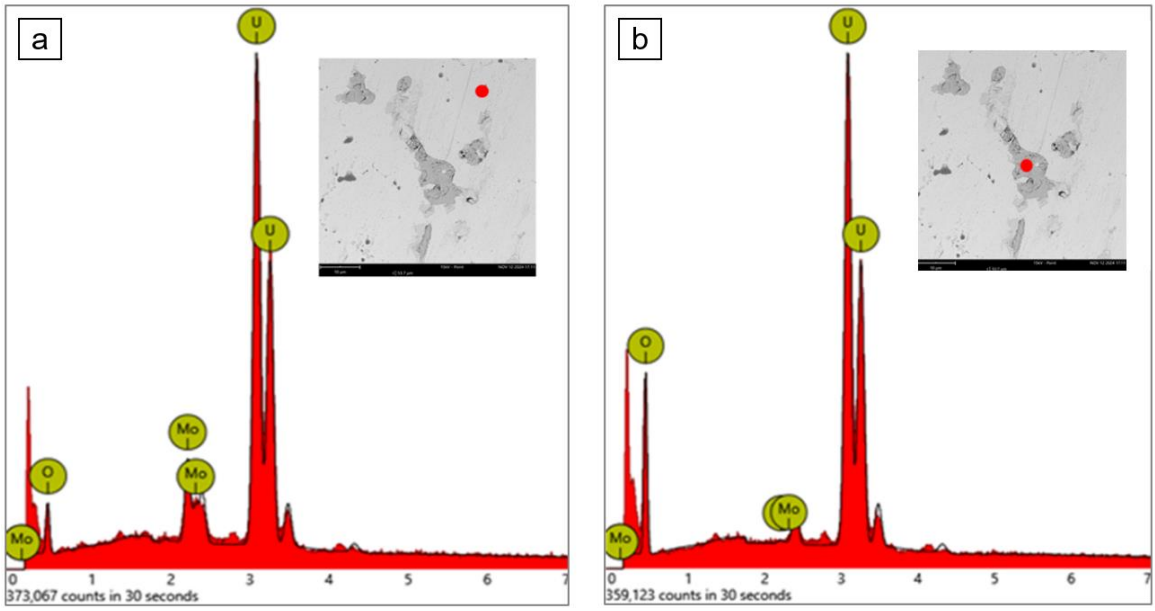


Figure 5. Elemental composition analysis of the bright (a), and dark region (b) using EDS.

## CONCLUSIONS

Density testing on U-7Mo, U-8Mo, and U-9Mo showed values consistent with theoretical densities, indicating minimal oxidation and porosity during the melting process. XRD results confirmed that the formed phase was γ-U without the presence of other phases. SEM-EDS analysis revealed bright and dark patterns in the alloy's microstructure, where the bright regions were Mo-rich but contained less oxide.

## ACKNOWLEDGEMENTS

This research was supported by funding from the Research and Innovation for Advanced Indonesia (RIIM) Competition program, provided by the Endowment Fund for Education Agency (LPDP) Ministry of Finance of the Republic of Indonesia and the National Research and Innovation Agency (BRIN). The contract numbers are B-3846/II.7.5/FR.06.00/11/2023 and B-7416/III.2/KU.06.04/11/2023, dated November 27, 2023, regarding the Implementation of the Research and Innovation for Advanced Indonesia Program, Batch 4.

We also express our gratitude to the staff of the Research Center for Nuclear Material and Radioactive Waste Technology, as well as the Directorate of Nuclear Facility Management, for their support in this research..

## REFERENCES

[1]. D. Sean O'Kelly, "An Introduction to Research Reactors," dalam *Encyclopedia of Nuclear Energy*, Elsevier, 2021, hlm. 1–7. doi: 10.1016/B978-0-12-819725-7.00054-4.

[2]. N. Pessoa Barradas, "Applications of Research Reactors," dalam *Encyclopedia of Nuclear Energy*, Elsevier, 2021, hlm. 8–25. doi: 10.1016/B978-0-12-819725-7.00110-0.

[3]. A. J. Cramer *dkk.*, "An investigation of the reaction of metallic uranium with oxygen/nitrogen gas mixtures," *Journal of Nuclear Materials*, vol. 584, hlm. 154564, Okt 2023, doi: 10.1016/j.jnucmat.2023.154564.

[4]. T. A. Pedrosa, A. M. M. Dos Santos, F. S. Lameiras, P. R. Cetlin, dan W. B. Ferraz, "Phase transitions during artificial ageing of segregated as-cast U–Mo alloys," *Journal of Nuclear Materials*, vol. 457, hlm. 100–117, Feb 2015, doi: 10.1016/j.jnucmat.2014.11.004.

[5]. S. Supardjo, A. Kadarjono, I. Isfandi, Y. D. A. Susanto, S. Permana, dan G. Guswardani, "Percobaan pembuatan pelat elemen bakar U-7Mo-xSi/Al dalam ukuran mini," *urania*, vol. 25, no. 3, Okt 2019, doi: 10.17146/urania.2019.25.3.5697.

[6]. W. Su, M. Pan, D. Mo, dan H. Xu, "Mechanical and thermal properties of

Mo for packaging HgCdTe IRFPA detector at cryogenic temperatures," *Infrared Physics & Technology*, vol. 127, hlm. 104373, Des 2022, doi: 10.1016/j.infrared.2022.104373.

[7]. S. R. Bacon, M. Brierley, M. A. Baker, dan J. F. Watts, "Oxidation of a depleted uranium-5 wt% molybdenum (U-5Mo) alloy in UHV by AES and XPS," *Surface & Interface Analysis*, vol. 51, no. 8, hlm. 849–856, Agu 2019, doi: 10.1002/sia.6659.

[8]. S. Van Den Berghe dan P. Lemoine, "Review of 15 years of high-density low-enriched UMo dispersion fuel development for research reactors in europe," *Nuclear Engineering and Technology*, vol. 46, no. 2, hlm. 125–146, Apr 2014, doi: 10.5516/NET.07.2014.703.

[9]. S. Octadamailah, A. Isnaini, dan R. Sigit, "Analisis kritikalitas proses hydriding serta penyimpanan paduan UMo dan UZr sebagai kandidat bahan bakar reaktor riset menggunakan OpenMC," *urania*, vol. 29, no. 1, hlm. 21, Apr 2023, doi: 10.17146/urania.2023.29.1.6976.

[10]. S. Octadamailah dan S. Supardjo, "Pengaruh densitas uranium terhadap umur bahan bakar nuklir di dalam reaktor RSG-GAS ditinjau dari aspek neutronik," *urania*, vol. 23, no. 2, Agu 2017, doi: 10.17146/urania.2017.23.2.3550.

[11]. V. P. Sinha, P. V. Hegde, G. J. Prasad, G. K. Dey, dan H. S. Kamath, "Effect of molybdenum addition on metastability of cubic γ-uranium," *Journal of Alloys and Compounds*, vol. 491, no. 1–2, hlm. 753–760, Feb 2010, doi: 10.1016/j.jallcom.2009.11.060.

[12]. K. Huang, Y. Park, D. D. Keiser, dan Y. H. Sohn, "Interdiffusion between potential diffusion barrier Mo and U-Mo metallic fuel alloy for RERTR applications," *J. Phase Equilib. Diffus.*, vol. 34, no. 4, hlm. 307–312, Agu 2013, doi: 10.1007/s11669-013-0236-z.

[13]. R. M. Hengstler *dkk.*, "Physical properties of monolithic U8wt.%–Mo," *Journal of Nuclear Materials*, vol. 402, no. 1, hlm. 74–80, Jul 2010, doi: 10.1016/j.jnucmat.2010.04.024.

[14]. P. E. Tomaszewski, "Structural phase transitions in crystals. I. Database," *Phase Transitions*, vol. 38, no. 3, hlm. 127–220, Mei 1992, doi: 10.1080/01411599208222899.

[15]. C. J. Humphreys, "The significance of Bragg's law in electron diffraction and microscopy, and Bragg's second law," *Acta Crystallogr A Found Crystallogr*, vol. 69, no. 1, hlm. 45–50, Jan 2013, doi: 10.1107/S0108767312047587.

[16]. F. G. Di Lemma *et al.*, "Annealing influence on the microstructure of irradiated U-Mo monolithic fuel foils," *Nuclear Materials and Energy*, vol. 35, hlm. 101436, Jun 2023, doi: 10.1016/j.nme.2023.101436.

THIS PAGE INTENTIONALLY LEFT BLANK

 DOI: https://doi.org/10.55981/Urania.2025.10793